Parametric Examination including Brief Survey of Composite and Homogenous Closed Ended Cylindrical Pressure Vessels

JACOB NAGLER

Faculty of Aerospace Engineering,
Technion,
Haifa 32000
ISRAEL
syanki@tx.technion.ac.il, syankitx@Gmail.com

Abstract:- This paper presents parametric design examination together with brief survey of composite and homogenous cylindrical pressure vessels with hemispherical ends. Two main kinds of composite and homogenous cylinders geometry were modeled and examined: thin and thick cylinders. Stress-strain relationships of the cylinders have been derived as a result of their model equation solution. Additionally, reinforced wrapping method effect on thin cylinder strength was presented and examined. Also, compound cylinder theory was discussed and main results were presented. Moreover, thick walled composite cylinders in polar coordinates theory has been developed and displayed together with other filament winding methods through analytic modeling and numerical examination. Finally, failure criteria of composed and homogenous cylinders were presented.

Keywords:- Composite, Homogenous, Cylinder, Pressure vessel, Closed ended, Filament wound.

I. Introduction

Pressure vessels are in use for a long time. Usually, the production of pressure vessels was done from only one specific material (ceramic or wood in ancient period while metal or alloy in modern times). During the years, more and more technology applications have made it possible to produce vessels from more than one material. Military and aerospace industry special products requirements of high strength and light-weight have lead (together with other reasons) to the use of composite materials. For example, on today's aerospace market 30-50% of the modern airplane structural components are made of composite materials. In particular, cylindrical or other vessels components which are usually have been manufactured by filament winding. Although they appear to be simple structures, composite and homogenous (non-composite material) cylinders (or other kinds of pressure vessels) are among the most difficult to design. Filament-wound composite pressure vessels have found widespread use not only for military use but also for civilian applications.

Pressure vessel is a closed container designed to hold gases and/or liquids at a pressure substantially different from the ambient pressure. The pressure differential is dangerous and fatal accidents have occurred in the history of pressure vessel development and operation. Consequently, pressure vessel design, manufacture, and operation are regulated by engineering authorities backed by legislation. For these reasons, the definition of a pressure vessel varies from country to country, but involves parameters such as maximum safe operating pressure and temperature. Pressure vessels are used in a variety of applications like aerospace engineering (airplane-cabin, fuel-chamber and engine-chamber), mechanical engineering (pneumatic and hydraulic reservoirs), chemical engineering (oil refinery and distillation towers), etc.

Pressure vessels can theoretically have almost any shape – the prevalent section

shapes are of spheres, cylinders and cones. A common design is a cylinder with end caps called 'heads'. Head shapes are frequently either hemispherical or dished (tori-spherical). More complicated shapes have historically been much harder to analyze for safe operation and are usually far more difficult to construct. Theoretically, a spherical pressure vessel has approximately twice the strength of a cylindrical pressure vessel with the same wall thickness [1]. Although spherical shapes are difficult to produce, and therefore more expensive, so most pressure vessels are cylindrical with 2:1 semi-elliptical heads or end caps on each end.

Theoretically, almost any material with good tensile properties that is chemically stable in the chosen application could be employed. However, pressure vessel design codes and application standards (see App. - Table A.1.) contain long lists of approved materials with associated limitations in temperature range.

Despite the growing use of composite materials, pressure vessels which are made of steel are still relevant. To manufacture a cylindrical or spherical pressure vessel, rolled and possibly forged - parts would have to be welded together. Some mechanical properties of steel achieved by rolling or forging, could be adversely affected by welding, unless special precautions are taken. In addition, current standards dictate the use of steel with a high impact resistance, especially for vessels used in low temperatures. In applications where carbon steel would suffer corrosion, special corrosion resistant material should also be used.

Some pressure vessels which are made of composite materials, such as filament wound composite using carbon fiber are held in place with a polymer. Due to the very high tensile strength of carbon fiber these vessels can be very light, but are much more difficult to manufacture. The composite material may be wound around a metal liner, forming a composite overwrapped pressure vessel.

In order to prevent leaking and protect the structure of the vessel from the contained medium, pressure vessels may be lined with various materials like metals, ceramics, or polymers. This liner may also carry a significant portion of the pressure load [2 -3].

Pressure vessels may also be constructed from concrete (PCV) or other materials which are weak in tension. Cabling, wrapped around the vessel or within the wall or the vessel itself, provides the necessary tension to resist the internal pressure. A "leak-proof steel thin membrane" lines the internal wall of the vessel. Such vessels can be assembled from modular pieces and so have "no inherent size limitations" [4]. There is also a high order of redundancy thanks to the large number of individual cables resisting the internal pressure.

Analytical solution for stress field development in thin or thick walled non-composite (homogenous) pressure vessels were made by R. Budyans *et al.* [5]. In cases where composite vessels calculations are more complicated, Gibson [6], Kaw [7], Kollar and Springer [8], Baker *et al.* [9] and others have laid the fundamentals of such calculations.

On the one hand, composite vessels are lightweight and with higher strength in the relevant directions than steel or aluminum counter-parts. On the other hand, manufacturing methods can be more complex and expensive than metallic counterparts.

This paper presents stress-strain relationships models of composite and homogenous cylindrical vessels including their hemispherical ends.

II. Analytical Model of Homogenous Cylindrical Vessel with Hemispherical Ends

The circular cylinder can be classified into two types: thick walled cylinder and thin walled cylinder. A thin walled

cylinder is a cylinder which his tangential stress (which is also called 'hoop stress' or 'circumferential stress') is inversely proportional to the thickness and is directly proportional to the inner radius. Also, the tangential stress should be developed in specified limits. The transition from "thin" to "thick" definition occurs asymptotically when the inner radius is no longer 10 times ('thumb rule') greater than the thickness of the cylinder. As a result, tangential and radial stresses are varied non-linearity with inner radius. In the following sections, these differences will be demonstrated, beginning with thin walled cylinder subject.

A. Thin Walled Cylinder with Hemispherical Ends

Stress field development in thin walled cylinder as appear in Fig. 1 is described broadly by Önder [10]. The main assumptions for using this method are:

1. Plane sections remain plane.
2. $r_i / t_c \geq 10$ ('Thumb-rule')
   with t_c being uniform constant cylinder thickness and r_i is the internal radius.
3. The applied pressure is the internal pressure only, p_i (since external pressure may cause buckling of the wall).
4. Material is linear-elastic, isotropic and homogeneous.
5. No variation of stress distributions throughout the wall thickness.
6. Fluid density is negligible.
7. No rotation.
8. Hemispherical ends.

Tangential stress in the cylinder can be expressed by:

$$2r_i L p_i = 2\sigma_{\theta_c} t_c L, \quad \sigma_{\theta_c} = \frac{p_i r_i}{t_c}. \quad (1)$$

while L is the cylinder length.
Hence, the maximum tangential stress is:

$$\sigma_{\theta_c,\max} = \frac{p_i (r_i + t_c / 2)}{t_c}. \quad (2)$$

The longitudinal stress in the cylinder is calculated as follows:

$$\sigma_{l_c} 2\pi r_i t_c = p_i \pi r_i^2, \quad \sigma_{l_c} = \frac{p_i r_i}{2t_c}, \quad (3)$$

while the tangential stress in the hemispherical ends is expressed by:

$$2\pi r_i t_s \sigma_{\theta_s} = p_i \pi r_i^2,$$
$$\sigma_{\theta_s} = \frac{p_i r_i}{2t_s} = \sigma_{l_s} \quad , \quad (4)$$

where t_s is the spherical surface thickness. The longitudinal stress in the hemispherical ends σ_{l_s} has the same calculation as σ_{θ_s}. By the way, Eqs. (3-4) assumes $t_c^2 << 1$ in spherical surface calculation by $\sigma_{l_c} \pi \left[(r_i + t_c)^2 - r_i^2 \right] = \sigma_{l_c} \pi \left[2r_i t_c + t_c^2 \right] = p_i \pi r_i^2$, since t_c is small enough.

Using Eq. (4) calculation, the maximum tangential stress in the spherical ends is:

$$\sigma_{\theta_s,\max} = \frac{p_i (r_i + t_s / 2)}{2t_s}. \quad (5)$$

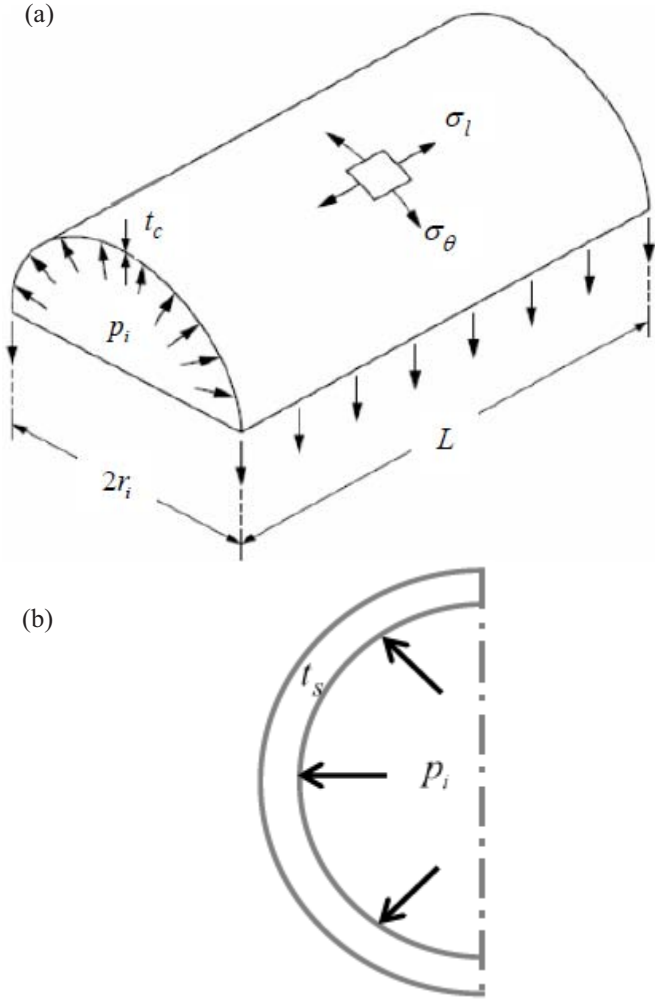

Figure 1. Thin cylindrical shell illustrations: a. Thin cylindrical shell with hemispherical ends – half section view. b. Cross section of hemispherical end ('Head').

It seems that if $t_s = t_c$, then tangential stress in the spherical ends is half of the tangential stress in the cylinder body. It's also true for the longitudinal stress. Moreover, longitudinal stress has no dependency in hemispherical thickness.

The relation between t_s and t_c is defined by hoop strain relations as follows:

$$\varepsilon_\theta = \underbrace{\frac{\sigma_{\theta_c} - \upsilon\sigma_{l_c}}{E}}_{\text{hoop strain of cylinder}} = \frac{p_i r_i}{2Et_c}(2-\upsilon) = \underbrace{\frac{\sigma_{\theta_s} - \upsilon\sigma_{l_s}}{E}}_{\text{hoop strain of hemispherical ends}} = \frac{p_i r_i}{2Et_s}(1-\upsilon), \quad \frac{t_s}{t_c} = \frac{1-\upsilon}{2-\upsilon}. \tag{6}$$

So, it seems that thickness ratio depends only on Poisson's ratio.

More about the joint region between cylinder and hemispherical ends can be studied from Bhaduri [14]. The strength of the cylinder component is dependent on joint efficiency (like welding or riveted joints/nails, etc). This efficiency is expressed in the thin layer model by using efficiency constant η with Eqs. (1, 3-4) as follows:

$$\sigma_{l_c} = \frac{p_i r_i}{2\eta_c t_c}, \quad \sigma_{\theta_c} = \frac{p_i r_i}{\eta_l t_c}, \quad \sigma_{\theta_s} = \frac{p_i r_i}{2t_s \eta_s}, \tag{7}$$

while η_c, η_l, η_s denote efficiencies of tangential, longitudinal and spherical joints, respectively.

On the one hand, it can be observed from Eqs. (3-4) that thickness increasing causes tangential stress decreasing which is excellent for material strength. On the other hand, it results in an increase in density, which means that more mass for the aircraft or rocket payload is added. Realization of this problem may lead to geometrical trade-off change in geometrical ends, or in the general shape, which would have a positive effect on decreasing mass and strength. For example, it's well known [5,11] that spherical shape yields equality between longitudinal and tangential stresses. The 'pay' for this kind of shape takes place in manufacturing methods which are very expensive. This later proposal of changing total geometry won't be checked in this essay. Alternatively, using other materials and different thickness ratios (wrapping methods) will be examined. In the next section, the thickness aspect will be discussed in the context of thick wall cylinder.

B. Thick Walled Cylinder with Hemispherical Ends

In case where the former assumption ('thumb rule') of ratio between thickness and inner radius ratio doesn't exist where $r_i / t_c < 10$ (see Fig. 2.a), we will use the following procedure. The relevant assumptions of this case are:

1. Plane sections remain plane.

2. $r_i / t_c < 10$ with t_c being uniform constant cylinder thickness and r_i is the internal radius.
3. Uniform internal (p_i) and/or external (p_o) pressure.
4. Deformation is symmetrical about z axis.
5. Material is linear-elastic, isotropic and homogeneous.
6. Fluid density is negligible.
7. No rotation.
8. Hemispherical ends.

Firstly, general polar equations of element equilibrium using Fig. 2.b will be written:

$$\begin{aligned} \hat{r}: \ & \frac{\partial \sigma_r}{\partial r}+\frac{1}{r}\frac{\partial \tau_{r\theta}}{\partial \theta}+\frac{\sigma_r-\sigma_\theta}{r}+F_r=0 \\ \hat{\theta}: \ & \frac{1}{r}\frac{\partial \sigma_\theta}{\partial \theta}+\frac{\partial \tau_{r\theta}}{\partial r}+\frac{2\tau_{r\theta}}{r}+F_\theta=0 \end{aligned} \quad . \qquad (8)$$

while σ_r and σ_θ denote the tangential and radial stresses acting normal to the sides of the element. F_r, F_θ represent the radial and tangential body forces, respectively. Since fluid density is neglected and no rotation is exist (assumptions 6 + 7), it can be concluded that $F_r = F_\theta = 0$. Moreover, shear stress fulfills that $\tau_{r\theta} = 0$ due to symmetrical deformation around z axis (assumption 2). All these assumptions lead to one equilibrium equation in $\hat{r}$ direction only:

$$\frac{\partial \sigma_r}{\partial r}+\frac{\sigma_r-\sigma_\theta}{r}=0, \qquad (9)$$

while strains behave according to Hook's law by:

$$\begin{aligned} \varepsilon_r &= \frac{\partial u}{\partial r}=\frac{1}{E}\left(\sigma_r-\upsilon\sigma_\theta\right) \\ \varepsilon_\theta &= \frac{u}{r}=\frac{1}{E}\left(\sigma_\theta-\upsilon\sigma_r\right) \\ \gamma_{r\theta} &= \frac{1}{r}\frac{\partial u}{\partial \theta}=\frac{1}{G}\tau_{r\theta}=0 \end{aligned} \quad . \qquad (10)$$

where u is the radial direction displacement. E, G represent modulus Young and shear modulus, respectively. υ is Poisson's ratio. Solving Eq. (10) for stress field yields the following relations:

$$\begin{aligned} \sigma_r &= \frac{E}{1-\upsilon^2}\left(\varepsilon_r+\upsilon\varepsilon_\theta\right)=\frac{E}{1-\upsilon^2}\left(\frac{\partial u}{\partial r}+\upsilon\frac{u}{r}\right) \\ \sigma_\theta &= \frac{E}{1-\upsilon^2}\left(\varepsilon_\theta+\upsilon\varepsilon_r\right)=\frac{E}{1-\upsilon^2}\left(\frac{u}{r}+\upsilon\frac{\partial u}{\partial r}\right) \end{aligned} \qquad (11)$$

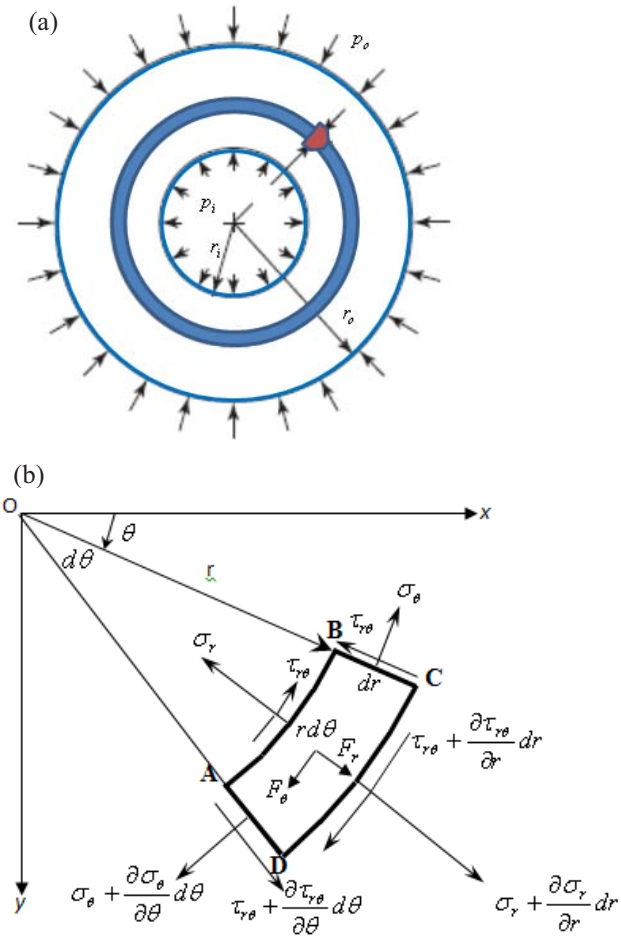

Figure 2. a. Thick cylindrical subjected to both internal and external pressure. b. Stress element in polar coordinates system.

Substituting the above relations (11) into equilibrium Eq. (9) results in the following radial displacement equation:

$$\frac{\partial^2 u}{\partial r^2}+\frac{1}{r}\frac{\partial u}{\partial r}-\frac{u}{r^2}=0 \qquad (12)$$

with B.C.: $\left(\sigma_r\right)_{r=r_i}=-p_i, \left(\sigma_r\right)_{r=r_o}=-p_o$

The solutions of for stress field and radial displacement by solving Eq. (12) using (11) are:

$$u=\left(\frac{1-\upsilon}{E}\right)\left(\frac{r_i^2 p_i - r_o^2 p_o}{r_o^2 - r_i^2}\right)r + \left(\frac{1+\upsilon}{E}\right)\frac{p_i - p_o}{r_o^2 - r_i^2}\left(\frac{r_o r_i}{r}\right)^2$$
$$\sigma_r = \frac{r_i^2 p_i - r_o^2 p_o}{r_o^2 - r_i^2} - \frac{p_i - p_o}{r_o^2 - r_i^2}\left(\frac{r_o r_i}{r}\right)^2 \quad (13)$$
$$\sigma_\theta = \frac{r_i^2 p_i - r_o^2 p_o}{r_o^2 - r_i^2} + \frac{p_i - p_o}{r_o^2 - r_i^2}\left(\frac{r_o r_i}{r}\right)^2$$

In case where each of these pressures (p_i or p_o) acts alone, qualitative stress distributions are shown in Fig. 3. Also, quantitative stress distributions are shown in Fig. 4.a-b for $r_o / r_i = 8$.

Since we deal with hemispherical ends which takes reactions from internal and external pressures (p_i and p_o), the longitudinal direction needs to be considered. By simple calculation we get the following expression for cylinder longitudinal stress:

$$\sigma_{l_c}\pi\left(r_o^2 - r_i^2\right) = p_i\pi r_i^2 - p_o\pi r_o^2,$$
$$\sigma_{l_c} = \frac{p_i r_i^2 - p_o r_o^2}{r_o^2 - r_i^2} \quad . \quad (14)$$

Additionally, longitudinal stress in the thick cylinder ends is (using hemispherical surface area - $2\pi r^2$):

$$\sigma_{l_s} 2\pi r_i\left(r_s - r_i\right) = p_i\pi r_i^2 - p_o\pi r_s^2,$$
$$\sigma_{l_s} = \frac{p_i r_i^2 - p_o r_s^2}{2r_i\left(r_s - r_i\right)} = \sigma_{\theta_s} \quad . \quad (15)$$

while σ_{θ_s} represents the tangential stress in the hemispherical end, and r_s is the spherical outer radius ($r_i + t_s$).

Table 1. Maximum radial stress value according to Eq. (13).

Internal and External pressures ratios	r	$\sigma_{r,\max}$
$p_i > p_o$	$r = r_i$	p_i
$p_o > p_i$	$r = r_o$	p_o

It seems from Table.1 that the maximum radial stress value according to Eq. (13) is obtained for $r = r_i$ while $p_i > p_o$. Otherwise ($p_i < p_o$), the maximum radial stress is obtained for $r = r_o$ and equals p_o.

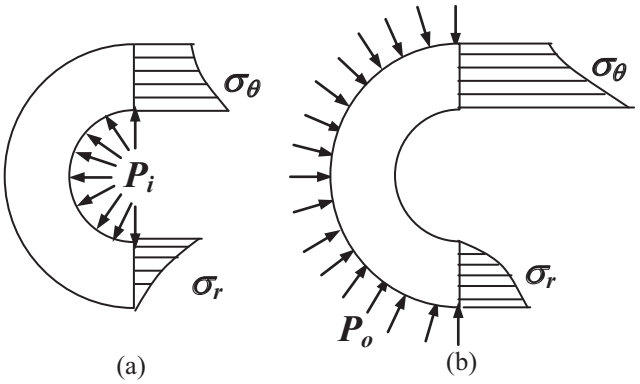

Figure 3. a. Qualitative stress and displacement distribution section map of thick cylinder subjected to internal pressure. b. Qualitative stress and displacement distribution section map of thick cylinder subjected to external pressure.

Separate discussion on the maximum tangential stress which occurs at either the inner, or outside edge according to pressure ratio, will be elaborated here. According to Ugural and Fenster [13], tangential stress limitations of thick cylinders were studied firstly by Ranov and Park [15]. The examination will be divided into three parts: (1) Internal pressure only, (2) External pressure only and both (3) Internal & External pressures. In cases (1) + (2), the maximum tangential stress is obtained at $r = r_i$ as shown in Table. 2, but there are several other cases when both pressures are acting while the maximum tangential stress is obtained at $r = r_o$. In order to investigate those cases, we will use the following notation according to [13]:

$$\sigma_\theta = p_i\frac{1 - PR^2}{R^2 - 1} + p_i\left(\frac{r_o}{r}\right)^2\frac{1 - P}{R^2 - 1}, \quad (16)$$
$$P = \frac{p_o}{p_i},\ R = \frac{r_o}{r_i}$$

Hence,

$$S = \frac{\sigma_{\theta i}}{\sigma_{\theta o}} = \frac{1 - 2PR^2 + R^2}{2 - PR^2 - P}. \quad (17)$$

The maximum value magnitude for tangential stress is obtained at the red ($S = 1$) and the purple ($S = 0$) dashed lines

in the outer surface region ($r = r_o$) as shown in Fig.4.c. The absolute displacement distributions graphs for both internal and external pressures are exhibited in Fig.4.d. These graphs behavior fits with tangential and radial stress behavior. Excellent result compatibility and sustaining was found between Ugural & Fenster [13] results and Fig. 4.

Comparison between thick cylinder to thin cylinder, in case where only internal pressure operates (since buckling can occur in thin vessel with external pressure) leads to conclusion that σ_θ diminishes with thickness in thick cylinder because of denominator and numerator decreasing. By saying that

$$\sigma_\theta = \underbrace{\frac{p_i\left(r^2 + r_o^{\,2}\right)}{\left(r_o - r_i\right)\left(r_o + r_i\right)}\left(\frac{r_i}{r}\right)^2}_{\text{Thick cylinder}} < \underbrace{\frac{p_i r}{t}}_{\text{Thin cylinder}},$$

since $r_o - r_i > t$ and so $r_o + r_i > t$ is obtained. As a result, by using some algebraic manipulations, $\sigma_\theta\big|_{\text{Thick cylinder}} < \sigma_\theta\big|_{\text{Thin cylinder}}$ inequality is obtained.

Table 2. Maximum tangential stress value according to Eq. (13).

Case	r	$\sigma_{\theta,\max}$
Internal pressure only	$r = r_i$	$p_i \frac{r_o^{\,2} + r_i^{\,2}}{r_o^{\,2} - r_i^{\,2}}$
External pressure only	$r = r_i$	$-\frac{2r_o^{\,2} p_o}{r_o^{\,2} - r_i^{\,2}}$
Internal and External pressures	$r = r_i$ in the bald lines – Fig.4.c	See Fig.4
Internal and External pressures	$r = r_o$ in the dashed lines – Fig.4.c	See Fig.4

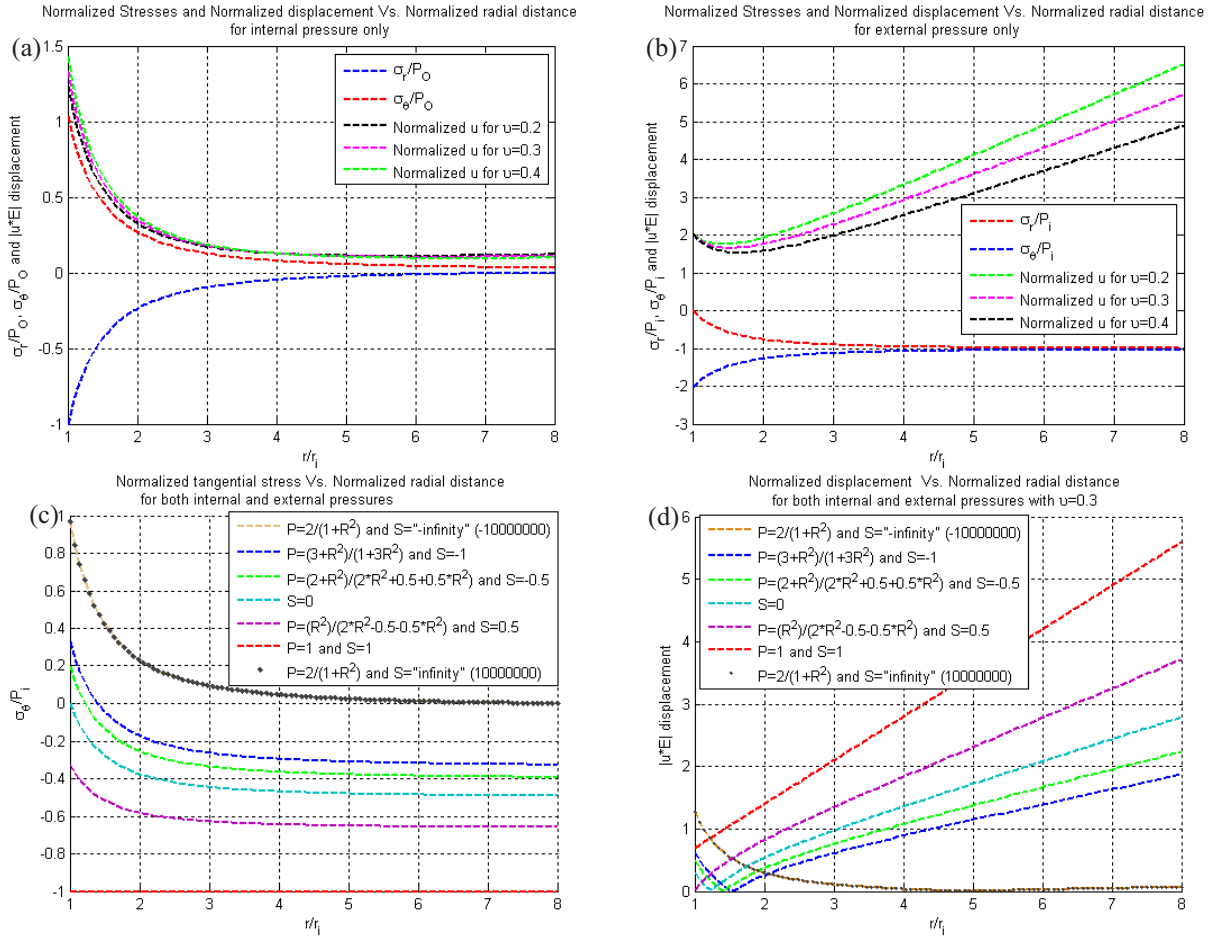

Figure 4. Illustrations for thick walled cylinder subjected to: a. Internal pressure – radial and tangential stresses and displacement distributions. b. External pressure – radial and tangential stresses and displacement distributions. c. Internal and external pressures – tangential distribution. d. Internal and external pressures – displacement distribution for $\upsilon = 0.3$.

C. Homogenous Cylindrical Vessel Failure Criteria

In this section, we will discuss the failure criteria of homogenous (non-composite material) cylindrical vessels. According to [13] there are five main criteria:

1. Maximum principal stress criterion assumes that material failure occurs when the maximum principal stress (σ_1) in a material element exceeds the uniaxial tensile strength of the material. Practically speaking, one should check the maximum stresses ($\sigma_{r,\max}, \sigma_{\theta,\max}, \sigma_{l,\max}$) according to relevant case (Thin-wall or Thick wall) and compare it to the material tensile elastic strength (yield stress - σ_{yp}):

$$\sigma_{r,\max} \text{ or } \sigma_{\theta,\max} \text{ or } \sigma_{l,\max} \le \sigma_{yp}. \quad (18)$$

Alternatively, this criterion can be used in order to calculate the desirable pressure value (p_o or p_i).

2. Maximum shearing stress criterion also known as *Tresca yield criterion* is often used to predict the yielding of ductile materials. Yield in ductile materials is usually caused by the slippage of crystal planes along the maximum shear stress surface. Therefore, a given point in the body is considered safe as long as the maximum shear stress at that point is under the yield shear stress τ_{yp} (which is usually half of the metal tensile yield stress - $\sigma_{yp}/2$) obtained from a uniaxial tensile test. This criterion should fulfill:

$$\tau_{\max} = \frac{\sigma_r - \sigma_\theta}{2} \le \tau_y. \quad (19)$$

Alternatively, it can be used to evaluate pressure values (p_o or p_i). This theory is used usually with brittle materials.

3. Energy of distortion theory proposes that the total strain energy can be separated into two components: the volumetric (hydrostatic) strain energy and the shape (distortion or shear) strain energy. It is proposed that yield occurs when the distortion component exceeds the strain at the tensile yield point for a simple tensile test. A formulated model for this theory is in the following form:

$$\sqrt{\sigma_r^2+\sigma_l^2+\sigma_\theta^2-2\left(\sigma_\theta\sigma_r+\sigma_l\sigma_r+\sigma_\theta\sigma_l\right)}\le\sigma_{yp}, \quad (20)$$

while all components of shear stress are zero (assumption).

Alternatively, this criterion can be used in order to calculate the desirable pressure value (p_o or p_i).

4. Maximum principal strain theory was proposed by St.Venant. According this theory, yield occurs when the maximum principal strain reaches the strain corresponding to the yield point during a simple tensile test. In terms of the principal stresses, it is determined by the following equation:

$$\sigma_\theta-\upsilon\left(\sigma_r+\sigma_l\right)\le\sigma_{yp}. \quad (21)$$

Alternatively, this criterion can be used in order to calculate the desirable pressure value (p_o or p_i).

5. Octahedral shearing stress theory will be defined with notes by Wolf *et al.* [16]. Octahedral plane cuts across one of the corners of a principal element, so that the eight planes together form an octahedron. Figure 5 illustrates the orientation of one of the eight octahedral planes which are associated with a given stress state. All 8 planes have identical normal stresses. Also, normal stresses don't deform the octahedron. Moreover, shear stresses are also with identical values and they may deform the octahedron without changing its total volume. The criterion importance is derived from the fact that octahedral shear stress is smaller than the highest principal shear stress, but it constitutes a single value that is influenced by all three principal shear stresses. The criterion is given by the following condition:

$$\tau_{oct}=\frac{\sqrt{\left(\sigma_\theta-\sigma_r\right)^2+\left(\sigma_r-\sigma_l\right)^2+\left(\sigma_l-\sigma_\theta\right)^2}}{3}\le\frac{\sigma_{yp}\sqrt{2}}{3}\approx\frac{\sigma_{yp}}{2} \quad (22)$$

while all shear stress components equals to zero (assumption). This criterion can be applied with all materials, since no material properties are involved.

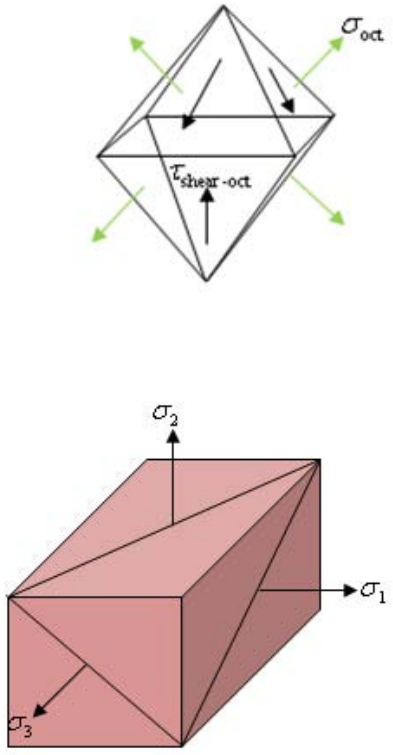

Figure 5. Octahedral Planes associated with a given stress state.

In conclusion, in order to understand failure mechanism, all failure criteria should be checked and compared one against each other. Usually, octahedral shearing stress criterion and energy of distortion criterion are coincided with each other (see also Ref. [13]).

III. Compound Cylinders

Compound cylinders are combined of two cylinders which supposed to be more effective by reducing tangential and radial stresses and to hold large pressures. There are several different methods of vessels

production, such as cooling & heating, wrapping methods, pressure compression methods, shrinking methods, extrusion, etc. The model calculation here assumes that both cylinders are made of two different materials with appropriate modulus Young and Poisson's ratio in the inside (E_i, υ_i) and outside (E_o, υ_o) cylinders, respectively. It is assumed that hemispherical ends will not be included in this section.

Suppose that external radius of the inner cylinder is larger than internal radius of the outer cylinder by difference of δ as shown in Fig.6.a.

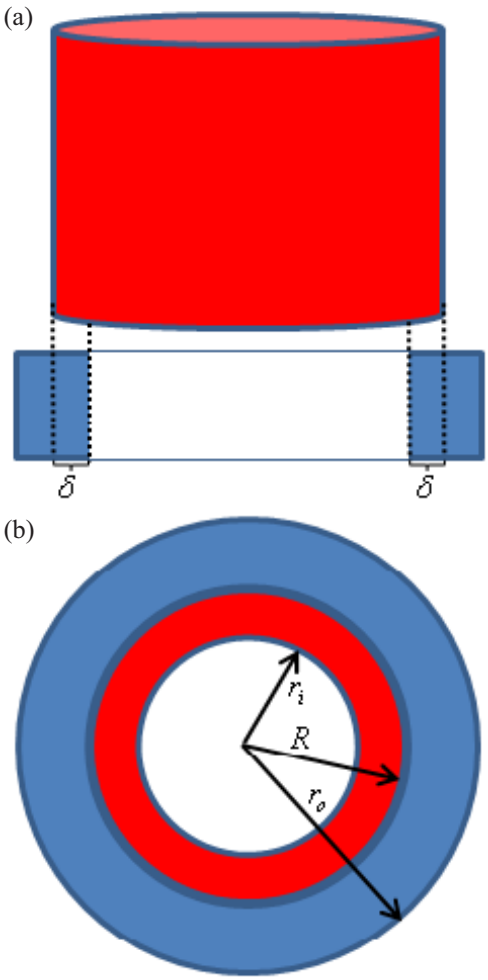

Figure 6. Compound cylinders sections: a. Before insertion. b. After insertion.

This phenomenon causes the outer cylinder to 'feel' an internal pressure. As a result of Newton's third law, the inner cylinder 'feels' an external pressure. Due to the radial interference δ between both outer and internal cylinders, an internal pressure contact is developed which causes to the following equilibrium of radial displacement:

$$u = \underbrace{u_{\text{inner cylinder}}}_{\text{External pressure}} + \underbrace{u_{\text{outer cylinder}}}_{\text{Internal pressure}} = \underbrace{\left(\frac{p_c R}{E_i}\right)\left(\frac{r_i^2+R^2}{r_i^2-R^2}-\upsilon_i\right)}_{r=R} + \underbrace{\left(\frac{p_c R}{E_o}\right)\left(\frac{r_o^2+R^2}{r_o^2-R^2}+\upsilon_o\right)}_{r=R} = \delta \quad (23)$$

while R is the nominal radius. Eq. (23) has been obtained using Eq. (13) for special cases (internal and external radial displacements) whereas p_i, p_o have been alternatively switched to interface pressure (p_c), respectively. Interface pressure contact can be isolated using Eq. (23) in the following form:

$$p_c = \frac{\delta}{\left(\frac{R}{E_i}\right)\left(\frac{r_i^2+R^2}{r_i^2-R^2}-\upsilon_i\right)+\left(\frac{R}{E_o}\right)\left(\frac{r_o^2+R^2}{r_o^2-R^2}+\upsilon_o\right)} \quad (24)$$

while all internal stresses $(\sigma_r, \sigma_\theta, \sigma_l)$ should be calculated according to cylinder pressure behavior (internal pressure or external pressure). Parameter optimization problem of compound cylinders were solved analytically and numerically for two and three layers with various constraints by Majzoobi & Ghomi [17] and by Miraje & Patil [18], respectively. Ref. [18] gives exact procedure for estimating the optimal order of the layers together with tangential stress expressions.

In addition, when the compound cylinder is subjected to a working pressure (internal pressure), a reacting pressure is developed at the contact surface of the mating cylinders and is given by [17]:

$$p_r = \frac{2p_i}{\left[\left(\frac{R}{r_i}\right)^2-1\right]\left[\frac{R^2+r_i^2}{R^2-r_i^2}+\frac{E_1}{E_2}\frac{r_o^2+R^2}{r_o^2-R^2}-\upsilon_1+\frac{E_1}{E_2}\upsilon_2\right]} \quad (25)$$

The pressures according to Eqs. (24-25) act as external pressures for the inner cylinder and as internal pressures for the outer cylinder. Hence, we get the following

relations for internal and external pressure vessel:

$$\begin{aligned}&\text{Internal layer: } p_i = \text{Working pressure}\\&\text{(internal pressure), } p_o = p_c + p_r \qquad (26)\\&\text{Outer layer: } p_o = 0, p_i = p_c + p_r\end{aligned}$$

while stresses in both cylinders will be calculated using Eqs. (13, 26).

The generalized theory of compound cylinder with n layers would be developed here, according to following procedure. Consider a general compound cylinder with concentric n cylinder layers as illustrates below in Fig.7. Each cylinder layer radius is noted by: $r_1, r_2, r_3, r_4 .. r_j, ..., r_n$ while j range fulfills $1 \le j \le n$. Therefore, the nominal radius r_j is represented by $j = 2, 4, .., .$ Each adjacent pair layers radial interference will be noted by $\delta_{1-2}, \delta_{2-3}, \delta_{3-4}, ... \delta_{k-1,k}, ..., \delta_{n-1,n}$ while $2 \le k \le n$.

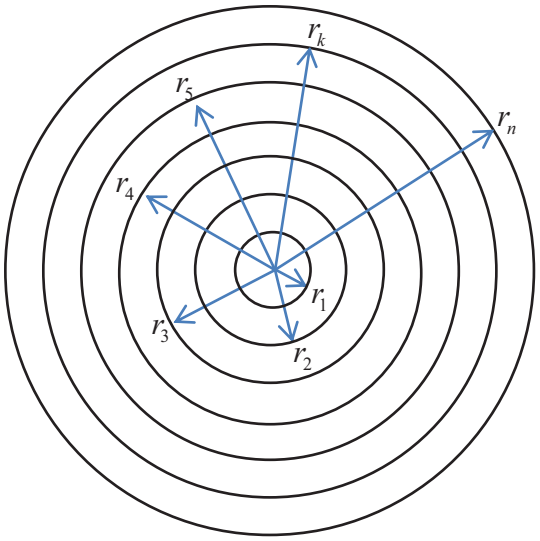

Figure 6. Compound cylinder with n cylinder layers.

Also, each layer has its own material properties such as $(E_1, \upsilon_1), (E_2, \upsilon_2), ..., (E_j, \upsilon_j), ...(E_n, \upsilon_n)$.

Further analytic examination of the problem would be divided into three main parts: (a) internal pressure inside the inner layer (p_i), (b) external pressure at outer layer (p_o), or (c) both internal and external pressures. This section presents only the first part examination (see explanation below). The solution for internal pressure at the inner layer is shown in Table. 3 below. Notice that solution of compound cylinders with external pressure only (b) is the same as in this case (a) with one distinction - calculation should begin from outer layer to the inner layer. For more information see Ref. [17-18]. The case of both external and internal pressure operating (c) is required more complicated calculations with convergence processes.

Table 3. General solution for compound cylinder subjected to internal pressure.

Layers	Radial interference (δ)	Contact pressure (p_c)
$1,2$	δ_{1-2} (given)	$p_{1-2}=\dfrac{\delta_{1-2}}{\left(\dfrac{r_2}{E_1}\right)\left(\dfrac{r_1^2+r_2^2}{r_1^2-r_2^2}-\upsilon_1\right)+\left(\dfrac{r_2}{E_2}\right)\left(\dfrac{r_3^2+r_2^2}{r_3^2-r_2^2}+\upsilon_2\right)}$
$2,3$	$\delta_{2-3}=u_1+u_2$	$p_{2-3}=\dfrac{\delta_{2-3}}{\left(\dfrac{r_3}{E_2}\right)\left(\dfrac{r_2^2+r_3^2}{r_2^2-r_3^2}-\upsilon_2\right)+\left(\dfrac{r_3}{E_3}\right)\left(\dfrac{r_4^2+r_3^2}{r_4^2-r_3^2}+\upsilon_3\right)}$
…	…	…
$k-1,k$	$\delta_{k-1,k}=u_{k-1}+u_k$ Should be calculated according Eq. (13)	$p_{k-1,k}=\dfrac{\delta_{k-1,k}}{\left(\dfrac{r_3}{E_2}\right)\left(\dfrac{r_2^2+r_3^2}{r_2^2-r_3^2}-\upsilon_2\right)+\left(\dfrac{r_3}{E_3}\right)\left(\dfrac{r_4^2+r_3^2}{r_4^2-r_3^2}+\upsilon_3\right)}$
Layers	σ_r and σ_θ due to contact pressure	
$1,2$	$\sigma_{r_1}\big\vert_{\text{Layer 1}}$ and $\sigma_{\theta_1}\big\vert_{\text{Layer 1}}$ (Substitute in Eq.(13): $p_{0_{1-2}}=p_{c_{1-2}}+p_{r_{1-2}},p_i,r_1,r_2$)	
$2,3$	$\sigma_r\big\vert_{\text{Layer 2}}$ and $\sigma_\theta\big\vert_{\text{Layer 2}}$ (Substitute in Eq.(13): $p_{0_{2-3}}=p_{c_{2-3}}+p_{r_{2-3}},p_i,r_2,r_3$)	
…	…	
$k-1,k$	$\sigma_r\big\vert_{\text{Layer }k}$ and $\sigma_\theta\big\vert_{\text{Layer }k}$ (Substitute in Eq.(13): $p_{o_{k-1,k}}=p_{c_{k-1,k}}+p_{r_{k-1,k}},p_{i_{k-1,k}}=p_{c_{m-2,m-1}}+p_{r_{m-2,m-1}},r_{k-1},r_k$) while $3\le m\le n$ and $2\le k\le n$	

IV. Composite Cylinders with Hemispherical Ends

This section presents analysis methods of composite cylinder. Cylinders which are formed using composite materials have been investigated for the last four decades. Two researchers from NASA Corporation, Nemeth and Mikulas [19] have been investigated stiffness and other laminated - composite cylinder parameters of buckling phenomenon. Furthermore, Tatting [20] has examined design parameters of variable stiffness composite cylinders. Since we are dealing with composite material, it will be useful to mention that there are four main types of composite materials structures: fiber, sandwich, honeycomb and multi – phases. For more information see Ref. [9,21].

This section will be focused on the following subjects:

- Wire wound thin cylinders with hemispherical ends.
- Thick walled composite cylinders in polar coordinates.
- Filament winding method estimation of composed cylinder.
- Failure criteria of composite materials.

A. Wire Wound Thin Cylinders with Hemispherical Ends

Wire wound thin cylinders which are also known as 'Wire wound thin cylinders' or 'Composite reinforcement'[23] are used to increase strength of thin cylinders to withstand high internal pressures without excessive increase in wall thickness as appear in Fig. 8. By using this method, weight and cost can be saved. Some ways of doing it use wound with high tensile steel tape or wire under tension. According to Hern [22], the reinforcement causes the cylinder to 'feel' an initial compressive hoop stress which must be overcome by the stresses owing to internal pressure before the material is subjected to tension. It remains at this stage before the

maximum allowable stress in the cylinder is exceeded. Calculating the tension that is developed in the tape during the winding process in order to ensure that the maximum hoop stress in the cylinder will not exceed a certain value, when the internal pressure is applied, will be performed here. This sub section takes step ahead with generalization of Hern's theory by regarding to hemispherical ends and initial internal pressure.

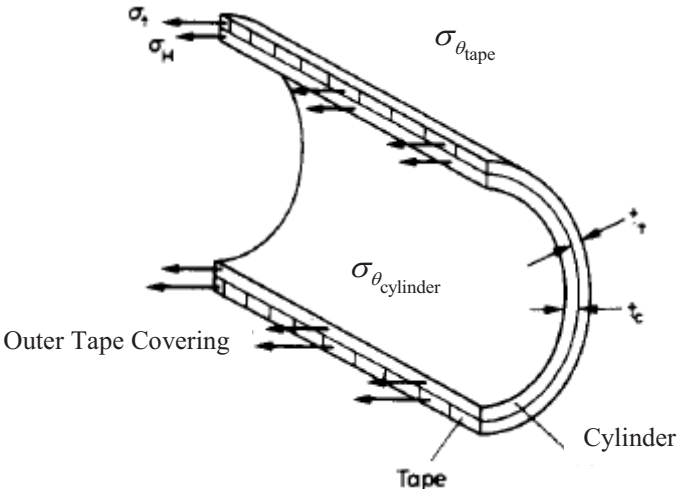

Figure 7. Section of a thin cylinder with an external layer of tape wound on with a tension.

The cylinder body initial state equilibrium is:

$$\underbrace{\sigma_{\theta,\text{tape}}\big|_{\text{initial}}\, 2Lt_{\text{tape}}}_{\text{Force due tape}} + \underbrace{\sigma_{\theta,\text{cylinder}}\big|_{\text{initial}}\, 2Lt_{\text{cylinder}}}_{\text{Resistive Cylinder Force}}, \quad = 2r_i L p_{i,1} \tag{27}$$

while $\sigma_{\theta,\text{tape}}$ represents the compressive stress, $p_{i,1}$ is the initial internal pressure, r_i - internal cylinder radius. $t_{\text{cylinder}}, t_{\text{tape}}$ represent the thicknesses of cylinder and tape, respectively.

The equilibrium after changing internal pressure is:

$$\sigma_{\theta,\text{tape}}\big|_{\text{final}}\, 2Lt_{\text{tape}} + \sigma_{\theta,\text{cylinder}}\big|_{\text{final}}\, 2Lt_{\text{cylinder}} = 2r_i L p_{i,f}, \quad p_{i,f} = p_{i,1} + p_{i,2} \tag{28}$$

while $p_{i,f}$ represents initial stress after adding, or subtracting $p_{i,2}$ pressure.

Equating differences of cylinder strain and tape strain in the tangential direction leads to the following relation:

$$\Delta\varepsilon_{\theta,\text{tape}} = \frac{\left(\sigma_{\theta,\text{tape}}\big|_{\text{final}} - \upsilon_{\text{tape}}\,\sigma_{l,\text{tape}}\big|_{\text{final}}\right) - \left(\sigma_{\theta,\text{tape}}\big|_{\text{initial}} - \upsilon_{\text{tape}}\,\sigma_{l,\text{tape}}\big|_{\text{initial}}\right)}{E_{\text{tape}}} = \Delta\varepsilon_{\theta,\text{cylinder}}$$
$$= \frac{\left(\sigma_{\theta,\text{cylinder}}\big|_{\text{final}} - \upsilon_{\text{cylinder}}\,\sigma_{l,\text{cylinder}}\big|_{\text{final}}\right) - \left(\sigma_{\theta,\text{cylinder}}\big|_{\text{initial}} - \upsilon_{\text{cylinder}}\,\sigma_{l,\text{cylinder}}\big|_{\text{initial}}\right)}{E_{\text{cylinder}}}. \tag{29}$$

while $\upsilon_{\text{cylinder}}$, υ_{tape} are the Poisson's ratio of cylinder and tape, respectively. Next step is to determine $\sigma_{\theta,\text{cylinder}}\big|_{\text{final}}$ using energy of distortion criterion (20):

$$\left(\sigma_{\theta,\text{cylinder}}\big|_{\text{final}}\right)^2 + \left(\sigma_{l,\text{cylinder}}\big|_{\text{final}}\right)^2 - \sigma_{l,\text{cylinder}}\big|_{\text{final}}\,\sigma_{\theta,\text{cylinder}}\big|_{\text{final}} \le \sigma_y{}^2. \tag{30}$$

Therefore, by solving Eqs. (27-30) together with longitudinal expression (3) we get the following relations for cylinder – tape region in Table. 4.

Table 4. General solution for wire wound thin cylinders case.

Case	$\sigma_{\theta,\text{cylinder}}$	$\sigma_{\theta,\text{tape}}$	$\sigma_{l,\text{cylinder}}$	$\sigma_{l,\text{tape}}$
Initial	$\dfrac{r_i p_{i,1} - \sigma_{\theta,\text{tape}}\big\|_{\text{initial}} t_{\text{tape}}}{t_{\text{cylinder}}}$	$\dfrac{\sigma_{\theta,\text{cylinder}}\big\|_{\text{final}}\left(\dfrac{t_{\text{cylinder}}}{t_{\text{tape}}} - \dfrac{E_{\text{tape}}}{E_{\text{cylinder}}}\right) + r_i\left(\dfrac{E_{\text{tape}}}{E_{\text{cylinder}}}\dfrac{p_{i,1}}{t_{\text{cylinder}}} - \dfrac{p_{i,f}}{t_{\text{tape}}}\right)}{1 - \dfrac{E_{\text{tape}}}{E_{\text{cylinder}}}\dfrac{t_{\text{tape}}}{t_{\text{cylinder}}}} + \dfrac{r_i\left(\dfrac{p_{i,1}-p_{i,f}}{2}\right)\left(\dfrac{\upsilon_{\text{tape}}}{t_{\text{tape}}} - \dfrac{E_{\text{tape}}}{E_{\text{cylinder}}}\dfrac{\upsilon_{\text{cylinder}}}{t_{\text{cylinder}}}\right)}{1 - \dfrac{E_{\text{tape}}}{E_{\text{cylinder}}}\dfrac{t_{\text{tape}}}{t_{\text{cylinder}}}}$	$\dfrac{p_{i,1}r_i}{2t_{\text{cylinder}}}$	$\dfrac{p_{i,1}r_i}{2t_{\text{tape}}}$
Final	$\dfrac{p_{i,f}r_i}{4t_{\text{cylinder}}} + \sqrt{{\sigma_y}^2 - 3\left(\dfrac{p_{i,f}r_i}{32t_{\text{cylinder}}}\right)^2}$	$\dfrac{\sigma_{\theta,\text{cylinder}}\big\|_{\text{final}} t_{\text{cylinder}} - r_i p_{i,f}}{t_{\text{tape}}}$	$\dfrac{p_{i,f}r_i}{2t_{\text{cylinder}}}$	$\dfrac{p_{i,f}r_i}{2t_{\text{tape}}}$

It's only left to examine the hemispherical ends stress behavior (especially, when very high pressures act, we want to strength the hemispherical ends). In similar way to the cylindrical body, the hemispherical initial state equilibrium is:

$$\underbrace{\sigma_{\theta_s,\text{tape}}\big|_{\text{initial}}\, 2\pi(r_i + t_{s,\text{tape}})t_{s,\text{tape}}}_{\text{Force due tape}} + \underbrace{\sigma_{\theta_s,\text{cylinder}}\big|_{\text{initial}}\, 2\pi r_i t_{s,\text{cylinder}}}_{\text{Resistive Cylinder Force}} = \pi r_i^2 p_{i,1} \quad (31)$$

,

while σ_{θ_s} represents the compressive stress and $p_{i,1}$ is the initial internal pressure.

The equilibrium after changing internal pressure is:

$$\sigma_{\theta_s,\text{tape}}\big|_{\text{final}}\, 2\pi(r_i + t_{s,\text{tape}})t_{s,\text{tape}} + \sigma_{\theta_s,\text{cylinder}}\big|_{\text{final}}\, 2\pi r_i t_{s,\text{cylinder}} = \pi r_i^2 p_{i,f},\ \ p_{i,f} = p_{i,1} + p_{i,2}\,. \quad (32)$$

Now, by equating between strain differences of hemispherical ends and hemispherical tape region, we obtain the following relation:

$$\Delta\varepsilon_{s,\text{tape}} = \frac{\left(\sigma_{\theta_s,\text{tape}}\big|_{\text{final}} - \upsilon_{\text{tape}}\,\sigma_{l_s,\text{tape}}\big|_{\text{final}}\right) - \left(\sigma_{\theta_s,\text{tape}}\big|_{\text{initial}} - \upsilon_{\text{tape}}\,\sigma_{l_s,\text{tape}}\big|_{\text{initial}}\right)}{E_{s,\text{tape}}} = \Delta\varepsilon_{s,\text{cylinder}}$$
$$= \frac{\left(\sigma_{\theta_s,\text{cylinder}}\big|_{\text{final}} - \upsilon_{\text{cylinder}}\,\sigma_{l_s,\text{cylinder}}\big|_{\text{final}}\right) - \left(\sigma_{\theta_s,\text{cylinder}}\big|_{\text{initial}} - \upsilon_{\text{cylinder}}\,\sigma_{l_s,\text{cylinder}}\big|_{\text{initial}}\right)}{E_{s,\text{cylinder}}} \quad . \quad (33)$$

Next stage is to determine $\sigma_{\theta_s,\text{cylinder}}\big|_{\text{final}}$ using energy of distortion criterion (20) such as:

$$\left(\sigma_{\theta_s,\text{cylinder}}\big|_{\text{final}}\right)^2 + \left(\sigma_{l_s,\text{cylinder}}\big|_{\text{final}}\right)^2 - \sigma_{l_s,\text{cylinder}}\big|_{\text{final}}\,\sigma_{l_s,\text{cylinder}}\big|_{\text{final}} \le {\sigma_y}^2\,. \quad (34)$$

Therefore, by solving Eqs. (31-34) together with longitudinal expression (4) we get the following expressions for spherical ends cylinder – tape region that are summarized in Table. 5.

Table 5. General solution for wire wound thin cylinders case.

Case	$\sigma_{\theta_s,\text{cylinder}}$	$\sigma_{\theta_s,\text{tape}}$	$\sigma_{l_s,\text{cylinder}}\Big\vert$	$\sigma_{l_s,\text{tape}}$
Initial	$\dfrac{r_i^2 p_{i,1} - \sigma_{\theta_s,\text{tape}}\Big\vert_{\text{initial}} 2(r_i + t_{s,\text{tape}})t_{s,\text{tape}}}{2r_i t_{s,\text{cylinder}}}$	See Eq. (35)	$\dfrac{p_{i,1} r_i}{2t_{s,\text{cylinder}}}$	$\dfrac{p_{i,1}\left(r_i + t_{s,\text{tape}}\right)}{2t_{s,\text{tape}}}$
Final	$\dfrac{p_{i,f} r_i}{4t_{s,\text{cylinder}}} + \sqrt{\sigma_y{}^2 - 3\left(\dfrac{p_{i,f} r_i}{32t_{s,\text{cylinder}}}\right)^2}$	$\dfrac{r_i^2 p_{i,f} - \sigma_{\theta_s,\text{cylinder}}\Big\vert_{\text{final}} 2r_i t_{s,\text{cylinder}}}{2(r_i + t_{s,\text{tape}})t_{s,\text{tape}}}$	$\dfrac{p_{i,f} r_i}{2t_{s,\text{cylinder}}}$	$\dfrac{p_{i,f}\left(r_i + t_{s,\text{tape}}\right)}{2t_{s,\text{tape}}}$

$$\sigma_{\theta_s,\text{tape}}\Big\vert_{\text{initial}} = \frac{\dfrac{r_i^2 p_{i,f} - \sigma_{\theta_s,\text{cylinder}}\Big\vert_{\text{final}} 2r_i t_{s,\text{cylinder}}}{2(r_i + t_{s,\text{tape}})t_{s,\text{tape}}} + \dfrac{\left(r_i + t_{s,\text{tape}}\right)\upsilon_{\text{tape}}}{2t_{s,\text{tape}}}\left(p_{i,1} - p_{i,f}\right)}{1 + \dfrac{E_{s,\text{tape}}}{E_{s,\text{cylinder}}}\dfrac{(r_i + t_{s,\text{tape}})t_{s,\text{tape}}}{r_i t_{s,\text{cylinder}}}} - \frac{\dfrac{E_{s,\text{tape}}}{E_{s,\text{cylinder}}}\left[\sigma_{\theta_s,\text{cylinder}}\Big\vert_{\text{final}} + \dfrac{\upsilon_{\text{cylinder}}}{2t_{s,\text{cylinder}}}\left(p_{i,1} - p_{i,f}\right)r_i - \dfrac{r_i^2 p_{i,1}}{2r_i t_{s,\text{cylinder}}}\right]}{1 + \dfrac{E_{s,\text{tape}}}{E_{s,\text{cylinder}}}\dfrac{(r_i + t_{s,\text{tape}})t_{s,\text{tape}}}{r_i t_{s,\text{cylinder}}}} \tag{35}$$

In order to simplify this theory, it can be assumed that $p_{i,1} = 0$. The reason for this assumption is because during winding process, or at the beginning of gas\liquid insertion, initial amount of gas\liquid pressure (initial state) is usually neglected (or not exists). Moreover, the whole development of Eqs. (27-35) represents transition from one state to another. Another simplification of calculation can be performed by assuming one equilibrium state, but only as long as the cylinder material has not yielded. Simplified stress-strain relations for one equilibrium state appear in Kunz notes [23]. However, this method can also be used for any other wrapping processes, not only for composite wrap.

(a)

(b)

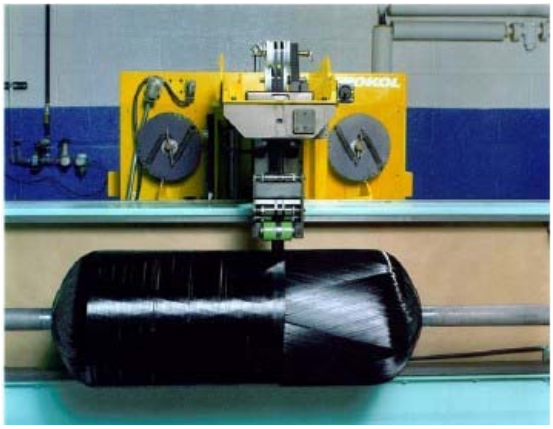

Figure 8. Filament winding of cylindrical tanks. a – Helical layers cover cylinders plus domes. b – Hoop plies cover cylinder section only. These photos are taken from Kunz notes [23].

B. Thick walled composite cylinders in polar coordinates

In this sub-section a polar coordinates approach to composite cylinder will be introduced and developed. Suppose, we have a general cylinder with inner radius r_i and outer radius r_o. Additionally, the cylinder is made of composite materials as illustrated in Fig. 9. Since averaged tangential elasticity modulus E_θ and averaged radial elasticity modulus E_r are functions of fibers number, they are not necessarily equal. The stress relations in polar coordinates are:

$$\begin{Bmatrix}\sigma_r\\ \sigma_\theta\end{Bmatrix}=\begin{bmatrix}E_r & E_{r\theta}\\ E_{\theta r} & E_\theta\end{bmatrix}\begin{Bmatrix}\sigma_r\\ \sigma_\theta\end{Bmatrix} \qquad (36)$$

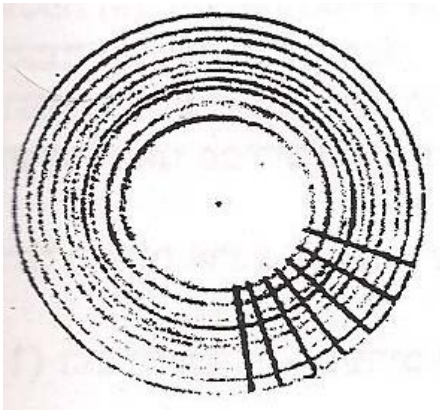

Figure 9. Thick walled composite cylinder.

while stress and strain field in more general form, including directions and stiffness characteristics are given by:

$$\begin{cases}\varepsilon_r=\dfrac{1}{E_r}\left(\sigma_r-\upsilon\sigma_\theta\right)\\ \varepsilon_\theta=\dfrac{1}{E_\theta}\left(\sigma_\theta-\upsilon\sigma_r\right)\end{cases}\rightarrow \qquad (37)$$
$$\begin{cases}\sigma_r=\dfrac{E_r}{1-\upsilon^2}\varepsilon_r+\dfrac{\upsilon E_\theta}{1-\upsilon^2}\varepsilon_\theta\\ \sigma_\theta=\dfrac{\upsilon E_r}{1-\upsilon^2}\varepsilon_r+\dfrac{E_\theta}{1-\upsilon^2}\varepsilon_\theta\end{cases}.$$

Substituting stresses according to Eq. (37) in equilibrium Eq. (9) yields:

$$\left[\frac{\partial E_{r\theta}}{\partial r}+\frac{E_{r\theta}-E_\theta}{r}\right]\varepsilon_\theta +\left[\frac{\partial E_r}{\partial r}+\frac{E_r-E_{r\theta}}{r}\right]\varepsilon_r+E_r\frac{\partial\varepsilon_r}{\partial r}=0 \qquad (38)$$

Substituting axis-symmetric polar coordinates strains expressions according to Eq. (10) into Eq. (38) leads to:

$$\left[\frac{\partial E_{r\theta}}{\partial r}+\frac{E_{r\theta}-E_\theta}{r}\right]\frac{u}{r}+ \left[\frac{\partial E_r}{\partial r}+\frac{E_r-E_{r\theta}}{r}\right]\frac{\partial u}{\partial r}+E_r\frac{\partial^2 u}{\partial r^2}=0 \qquad (39)$$

In case where $E_{r\theta}, E_r$ are constants we get the simple Euler' solution to Eq. (39) which is:

$$u = A_1 r^{k_1} + A_2 r^{k_2},$$
$$k_{1,2} = \frac{\frac{E_{r\theta}}{E_r} \pm \sqrt{\left(\frac{E_{r\theta}}{E_r}\right)^2 - 4\left(\frac{E_{r\theta} - E_\theta}{E_r}\right)}}{2}, \quad (40)$$

while A_1, A_2 are constants. It is easy to observe that if $E_{r\theta} = 0$ we get $k_{1,2} = \pm\sqrt{\frac{E_\theta}{E_r}}$.

In order to find enclosed formula for radial displacement and stress field, one should use B.C. as assumed in (12) together with (37) in order to calculate A_1, A_2 constants. This calculation can be easier using the following notation:

$$\frac{1}{1-\upsilon^2}\begin{bmatrix} E_r k_1 r_i^{k_1-1} + \upsilon E_{r\theta} r_i^{k_1} & E_r k_2 r_i^{k_2-1} + \upsilon E_{r\theta} r_i^{k_2} \\ E_r k_1 r_o^{k_1-1} + \upsilon E_{r\theta} r_o^{k_1} & E_r k_2 r_o^{k_2-1} + \upsilon E_{r\theta} r_o^{k_2} \end{bmatrix}\begin{Bmatrix} A_1 \\ A_2 \end{Bmatrix} = -\begin{Bmatrix} p_i \\ p_o \end{Bmatrix}$$
$$\rightarrow \quad (41)$$
$$\frac{1}{1-\upsilon^2}\begin{bmatrix} b_1 & b_2 \\ b_3 & b_4 \end{bmatrix}\begin{Bmatrix} A_1 \\ A_2 \end{Bmatrix} = -\begin{Bmatrix} p_i \\ p_o \end{Bmatrix}$$

Solving system (41) leads to the following constants definition:

$$A_1 = \left(\frac{1-\upsilon^2}{E_r}\right)\frac{p_o b_2 - p_i b_4}{b_1 b_4 - b_2 b_3},\ A_2 = \left(\frac{1-\upsilon^2}{E_r}\right)\frac{p_i b_3 - p_o b_1}{b_1 b_4 - b_2 b_3}. \quad (42)$$

Although it is required that the determinant will fulfill: $\begin{vmatrix} b_1 & b_2 \\ b_3 & b_4 \end{vmatrix} \neq 0$. In case where $E_{r\theta} = 0$ (when all fibers are given in tangential and radial direction only) we have:

$$\frac{E_r}{1-\upsilon^2}\begin{bmatrix} k_1 r_i^{k_1-1} & k_2 r_i^{k_2-1} \\ k_1 r_o^{k_1-1} & k_2 r_o^{k_2-1} \end{bmatrix}\begin{Bmatrix} A_1 \\ A_2 \end{Bmatrix} = -\begin{Bmatrix} p_i \\ p_o \end{Bmatrix}, \quad (43)$$

while

$$A_1 = \left(\frac{1-\upsilon^2}{E_r}\right)\frac{p_o r_i^{k_2-1} - p_i r_o^{k_2-1}}{k_1\left(r_i^{k_1-1} r_o^{k_2-1} - r_i^{k_2-1} r_o^{k_1-1}\right)},\ A_2 = \left(\frac{1-\upsilon^2}{E_r}\right)\frac{p_i r_o^{k_1-1} - p_o r_i^{k_1-1}}{k_2\left(r_i^{k_1-1} r_o^{k_2-1} - r_i^{k_2-1} r_o^{k_1-1}\right)}. \quad (44)$$

Hence, the expressions for radial displacement in the general form where $E_{r\theta} = 0$ is:

$$u = \left(\frac{1-\upsilon^2}{E_r}\right)\left[\frac{p_o r_i^{k_2-1} - p_i r_o^{k_2-1}}{k_1\left(r_i^{k_1-1} r_o^{k_2-1} - r_i^{k_2-1} r_o^{k_1-1}\right)} r^{k_1} + \frac{p_i r_o^{k_1-1} - p_o r_i^{k_1-1}}{k_2\left(r_i^{k_1-1} r_o^{k_2-1} - r_i^{k_2-1} r_o^{k_1-1}\right)} r^{k_2}\right]. \quad (45)$$

while stress should be derived using Eqs. (10, 37). Notice that since we deal with hollow cylinder the case where $r = 0$ is non-relevant. The longitudinal stresses calculations of cylinder and spherical ends will be performed using Eqs. (14-15), respectively. Generally, accurate calculation is achieved by considering spherical ends using longitudinal modulus as explained by Gibson [6]. If the spherical ends are made of composite material, the radial and tangential stresses should be calculated separately with composite method calculations or FEM (finite element methods) [24-25]. From here, we will pass to our next discussion about winding method estimation of composed cylinder.

C. Filament winding method estimation of composed cylinder

This sub section requires more deeply overview of the composite material theory. The reason for that is derived from the composite material complex behavior. Initially, we will start with understanding the winding method which is used to produce the composed cylinder. According to Önder [10],

there are three kinds of winding patterns as shown in Fig.10 and will be elaborated here.

- The first pattern is called *'Hoop Winding'* which is known as tangential or circumferential winding. Hoop winding is characterized by high helical angle of 90 [deg]. Each full rotation of the mandrel advances the band delivery by one full bandwidth as shown in Fig. 10.a.
- The second pattern is called *'Helical Winding*' which is done by mandrel rotation at a constant speed while the fiber feed carriage transverses back and forth at a speed regulated to generate the desired helical angles as shown in Fig. 10.b.
- The third pattern is called *'Polar Winding*' which is done by fiber passing tangentially to the polar opening at one end of the chamber, reverses direction, and passes tangentially to the opposite side of the polar opening at the other end using the mandrel arm rotation about the longitudinal axis as shown in Fig. 10.b. It is used to wind almost axial fibers on domed end type of pressure vessels. On vessels with parallel sides, a subsequent circumferential winding would be done.

Clear observation on these three winding patterns leads to helical winding process advantage with great versatility. Usually, cylinder vessel composite are produced by means of helical winding. In each pattern, one can vary winding tension, winding angle and/or resin content in each layer of reinforcement until desired properties such - thickness and strength of the composite are achieved. The properties of the finished composite can be varied by the type of winding pattern selected. Trading off wind angle and circuits to close the patterns can create any combination of diameter and length by wound.

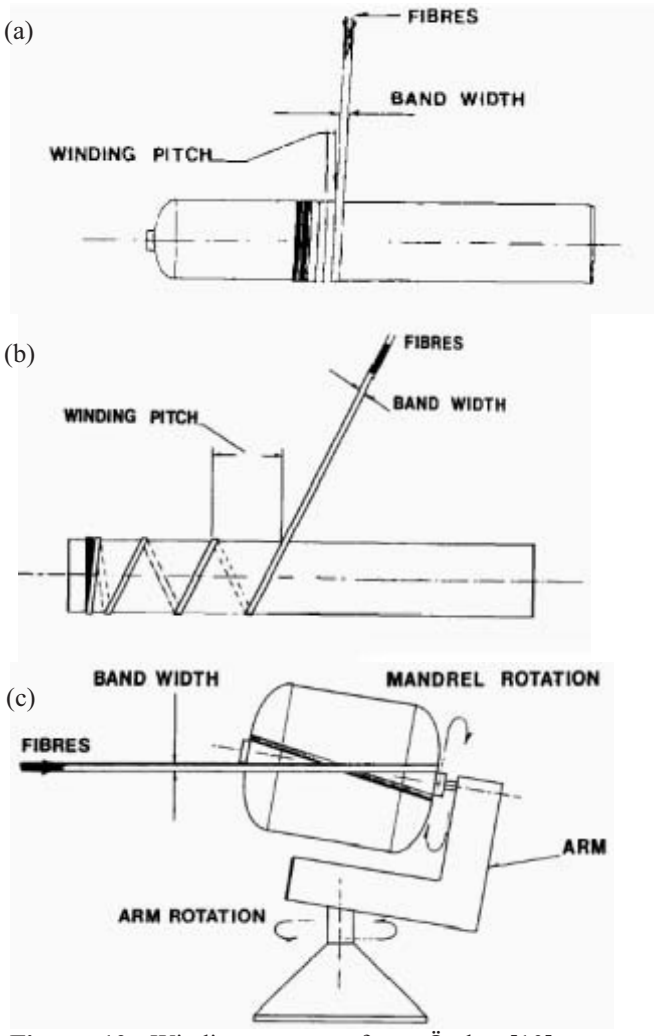

Figure 10. Winding patterns from Önder [10]. a. Hoop winding. b. Helical winding. c. Polar winding.

In order to understand better the importance of the filament wound composite in this field, we will take a brief look on the following tables from Ref. [10]. According to Table A.2 in the Appendix, it seems that the material properties of filament wound composite are similar to those of stainless steel or titanium alloy, with benefit of low density. Moreover, there are many applications of filament wound composite method according to Table. A.3.

After this brief introduction of filament wound composite, we have enough motivation to go forward with filament wound composite vessel mechanics. Firstly, a brief introduction of composite material structure will be displayed. Composite materials are usually heterogeneous and anisotropic material. Their uniqueness is in

their mechanical properties behavior which is changed from point to point; point in the matrix has different properties when compared to the fiber. Also, properties in one direction are not necessarily the same in other direction. These comprehensions are forced microscopic and macroscopic observations. The building block of the composite material structure is the lamina. The lamina usually consists of fiber/matrix configurations. The micromechanics view deals with mechanical behavior of constituent material, interactions between these kinds of materials and the resulting behavior of single lamina in a laminate as shown in Fig.11. However, macroscopic view concentrates in the gross mechanical behavior of composite materials structures (laminate) without regard to constituent materials and their internal interactions as shown in Fig.11. During the following discussion, stress-strain relationships between microscopic and macroscopic mechanics will be developed. General information concerning composite materials and particularly about lamina stress-strain relationships can be found in Ref. [6-9].

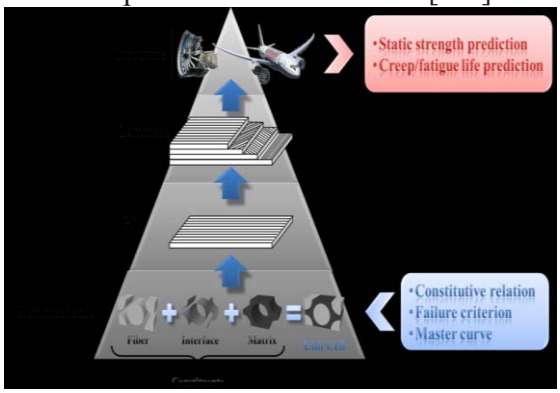

Figure 11. Micro-mechanics and Macro-mechanics perspectives of composite material (Wikipedia)

i. Thin Filament Wound Pressure Vessel

Suppose, we have a thin filament wound pressure vessel with non-principal coordinates (x, y) (body coordinates) and principal material coordinates $(1,2)$ as shown in Fig. 12-13.

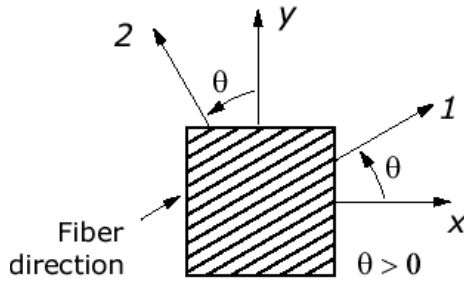

Figure 12. Lamina orientation in non-principal coordinates

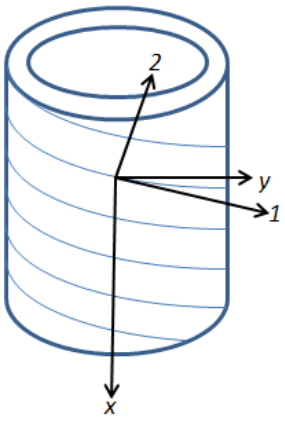

Figure 13. Filament wound pressure vessel in principal material coordinates

In order to find stress-strain relationships, coordinates transform from body coordinates (x, y) into principal material coordinates $(1,2)$ will be performed. The coordinate's orientation difference can be observed in Fig. 13. Also, it's assumed that only internal pressure acts (external pressure may cause buckling). Using Eqs. (1, 3) for thin cylinder leads to:

$$\sigma_x = \frac{p_i r_i}{2t_c},\ \sigma_y = \frac{p_i r_i}{t_c},\ \tau_{xy} = 0. \quad (46)$$

while these equations are assumed to be based on geometry and static equilibrium.

Since strain and stress are along fiber direction, we will pass to principal material coordinates $(1,2)$ by using orthotropic lamina theory [6]. The stress-strain transformation relationships from lamina coordinates to principal coordinates are:

$$\begin{Bmatrix}\sigma_1\\ \sigma_2\\ \tau_{12}\end{Bmatrix}=\begin{bmatrix}\cos^2\theta & \sin^2\theta & \sin 2\theta\\ \sin^2\theta & \cos^2\theta & -\sin 2\theta\\ -\frac{\sin 2\theta}{2} & \frac{\sin 2\theta}{2} & \cos 2\theta\end{bmatrix}\begin{Bmatrix}\sigma_x\\ \sigma_y\\ \tau_{xy}\end{Bmatrix},\quad (47)$$

$$\begin{Bmatrix}\varepsilon_1\\ \varepsilon_2\\ \gamma_{12}/2\end{Bmatrix}=\begin{bmatrix}\cos^2\theta & \sin^2\theta & \sin 2\theta\\ \sin^2\theta & \cos^2\theta & -\sin 2\theta\\ -\frac{\sin 2\theta}{2} & \frac{\sin 2\theta}{2} & \cos 2\theta\end{bmatrix}\begin{Bmatrix}\varepsilon_x\\ \varepsilon_y\\ \gamma_{xy}/2\end{Bmatrix}$$

Substituting relations (46) into (47) leads to the principal material stresses and strains as follows:

$$\{\sigma_1,\ \sigma_2,\ \tau_{12}\}=\frac{p_i r_i}{t_c}\left[\frac{1+\sin^2\theta}{2},\ \frac{1+\cos^2\theta}{2},\ \frac{\sin 2\theta}{4}\right] \quad (48)$$

In order to find strain relations we will use the following transformation instead of (47):

$$\begin{Bmatrix}\varepsilon_1\\ \varepsilon_2\\ \gamma_{12}\end{Bmatrix}=\begin{bmatrix}S_{11} & S_{12} & \\ S_{21} & S_{22} & \\ & & S_{66}\end{bmatrix}\begin{Bmatrix}\sigma_1\\ \sigma_2\\ \tau_{12}\end{Bmatrix},\quad (49)$$

$$\text{while } \sigma_3=\tau_{23}=\tau_{31}=0$$

where the compliances and the engineering constants are related by the following equations:

$$S_{11}=\frac{1}{E_1},\ S_{22}=\frac{1}{E_2},$$
$$S_{12}=S_{21}=-\frac{\nu_{21}}{E_2}=-\frac{\nu_{12}}{E_2},\ S_{66}=\frac{1}{G_{12}}. \quad (50)$$

Hence,

$$\{\varepsilon_1,\ \varepsilon_2,\ \gamma_{12}\}=\begin{bmatrix}\frac{1+\sin^2\theta}{2E_1}-\nu_{21}\left(\frac{1+\cos^2\theta}{2E_2}\right)\\ \frac{1+\cos^2\theta}{2E_2}-\nu_{21}\left(\frac{1+\sin^2\theta}{2E_2}\right)\\ \frac{\sin 2\theta}{4G_{12}}\end{bmatrix} \quad (51)$$

Resultant numerical analyzing of Eqs. (48, 51) leads to the following graphs using MATLAB program. While all stresses are normalized by $\frac{p_i r_i}{t_c}$. Also, strains of the first principal, second principal and shear are normalized by $\frac{p_i r_i}{t_c E_1}$, $\frac{p_i r_i}{t_c E_2}$, $\frac{p_i r_i}{t_c G_{12}}$, respectively. Notice that strain numerical calculation is based on the following data: $E_1=E_2$ and $\upsilon_{12}=0.25$.

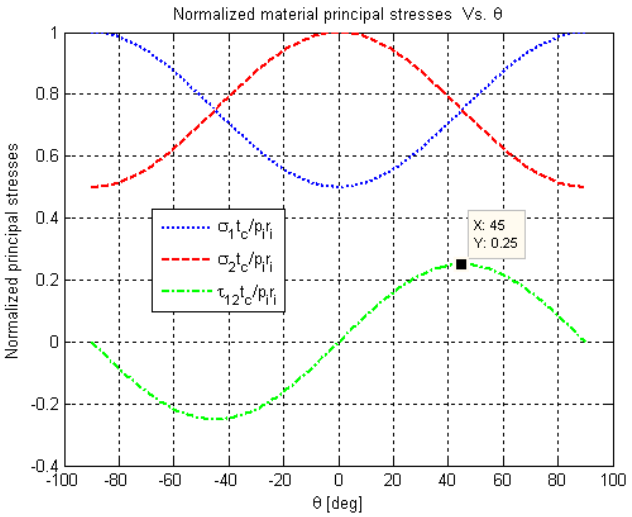

Figure 14. Normalized material principal stresses Vs. θ

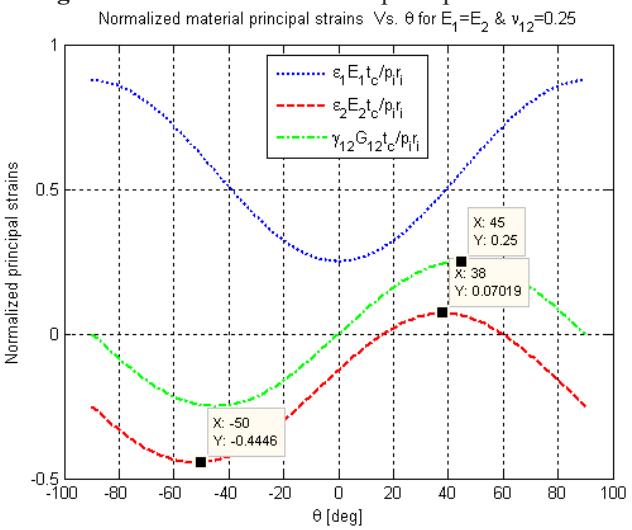

Figure 15. Normalized material principal strains Vs. θ

The following conclusions have been deduced using Fig.14-15:

- Maximum first principal stress and strain $(\sigma_{1,\max},\varepsilon_{1,\max})$ together with minimum second principal stress $(\sigma_{2,\min})$ are obtained at $\theta=-90^0,90^0$.

- Minimum first principal stress and strain ($\sigma_{1,\min}, \varepsilon_{1,\min}$) together with maximum second principal stress ($\sigma_{2,\max}$) are obtained at $\theta = 0^0$.
- First principal stress (σ_1) and second principal stress (σ_2) graphs are meet at $\theta = -45^0, 45^0$ (mutual angle).
- Minimum ($\tau_{12,\min}, \gamma_{12,\min}$) and maximum ($\tau_{12,\max}, \gamma_{12,\max}$) shear stresses and strains are obtained at $\theta = -45^0, 45^0$, respectively.
- Shear stress (τ_{12}) gets lowest value relative to first (σ_1) and second (σ_2) principal stresses.
- Maximum second principal strain ($\varepsilon_{2,\max}$) is obtained at $\theta = 38^0$, while its minimum value ($\varepsilon_{2,\min}$) is obtained at $\theta = -50^0$.
- The absolute strain values are fulfills: $\varepsilon_1 > \gamma_{12} > \varepsilon_2$ in each θ angle according to initial assumptions.

While all stresses and strains are normalized according to the remark above.

Spherical ends are divided into two groups: composites and homogenous. The case of homogenous spherical ends has been treated already in Sec.1. If the spherical ends are made of composite materials one should use 'The netting theory' which is beyond this essay discussion. For more information about this method see Ref. [26-29].

ii. Thick Filament Wound Pressure Vessel

Thick-walled composites vessels in three-dimensional coordinates were studied in detailed by Zu [30]. There are two types of methods for analyzing stress-strain relationships in thick-walled composites cylinder: (1) direct solution method and (2) stress function method. These methods are based on Lekhnitkii's theory [31-32] as brought by Önder [10], Tsukrov and Drach [33]. I suggest the reader to read about these methods in Zu study [30]. From here, we will pass to discuss our final subject on failure criteria of composite materials.

D. Failure criteria of composite materials

Failure criteria of composite materials have been discussed by [34-36] and others. There are two main criteria for failure of composite laminates.

- Maximum Stress (or strain) criteria – this theory emphasizes mode of failure but neglects the effect of stress interactions. This criterion is considered to be quite conservative (independent criterion). The following conditions must be satisfied in tension and/or shear:

$$\sigma_1 < F_t,\ \sigma_2 < G_t\ ,\ |\tau_{12}| < S_t, \qquad (52)$$

while F_t, G_t, S_t are the limiting tensile and shear strengths along principle material directions, respectively.

Moreover, in compression case the following condition must be satisfied:

$$\sigma_1 > F_c,\ \sigma_2 > G_c, \qquad (53)$$

while F_c, G_c are the limiting compressive strengths along principle material directions, respectively.

- Tsai-Wu failure theory (interactive criterion). This theory includes stress interactions in the failure mechanism and predicts first ply failure, but it requires some efforts to determine parameters. The mathematical formulation of this condition using [34] is:

$$F_{11}\sigma_1^{\,2} + 2F_{12}\sigma_1\sigma_2 + F_{22}\sigma_2^{\,2} + F_{66}\tau_{12}^{\,2} + F_1\sigma_1 + F_2\sigma_2 = 1, \qquad (54)$$

where,

$$F_{11} = \frac{1}{F_t F_c},\ F_{22} = \frac{1}{G_t G_c},\ F_{66} = \frac{1}{S^2}, \qquad (55)$$

$$F_1 = \frac{1}{F_t} - \frac{1}{F_c},\ F_2 = \frac{1}{G_t} - \frac{1}{G_c},\ F_{12} = -\frac{1}{2}\sqrt{F_{11}F_{22}}$$

while three dimensional generalize model of Tsai-Wu theory is presented by Bhavya *et al.* [36].

To sum it up, interactive theories which are based on curve fitting, like the Tsai-Wu criterion are preferable at predicting failure of a single lamina than independent criterion. However, in order to identify and understand failure mechanism, both methods should be used and compared against each other combined with FEM analysis.

V. Conclusion

Composites and homogenous cylinders with and without spherical ends were investigated. Each kind of cylinder was examined for thick and thin geometries according to the following order.

Analytical model of homogenous cylindrical vessel with hemispherical ends:

- Thin walled cylinder with hemispherical ends.
- Thick walled cylinder with hemispherical ends.
- Homogenous cylindrical vessel failure criteria.
- Compound cylinders.

Analytical model of composite cylindrical vessel with hemispherical ends:

- Wire wound thin cylinders with hemispherical ends.
- Thick walled composite cylinders in polar coordinates.
- Filament winding method estimation of composed cylinder:
  - Thin filament wound pressure vessel.
  - Thick filament wound pressure vessel.
- Failure criteria of composite materials.

Each of these subjects was presented and discussed. Additionally, all subjects were also examined analytically, not including thick filament wound pressure vessel subject. Numerical investigation using MATLAB program was done for thin filament wound pressure vessel subject. Moreover, qualitative and quantitative tests were presented for homogenous thick cylinder stress field. Each method has its own advantages and disadvantages in cost, manufacturing, strength and weight as appear in this text and the relevant references.

Acknowledgement

All figures in this article have been produced by the author of this study, not including Figures (8, 10 – 11) which have their own appropriate permissions. Fig. 8 and Fig.10 use permissions have been granted thanks to Prof. Richard Kunz and Prof. Dr. Onur Sayman, respectively. Fig. 11 has been granted permission by Wikipedia free-use rule.

References

[1] E. J. Hearn, *Mechanics of Materials 1: An Introduction to the Mechanics of Elastic and Plastic Deformation of Solids and Structural Materials*, 3rd Ed., Chapter 9: Butterworth-Heinemann., 1997 pp. 199–203.

[2] NASA Tech Briefs, *Making a Metal-Lined Composite Overwrapped Pressure Vessel*, Mar. 2005.

[3] O. Frietas, Maintenance and Repair of Glass-Lined Equipment, *Chemical Engineering. J*, Jul. 2007.

[4] D. Freyer and J. Harvey, *High Pressure Vessels*, 1998.

[5] R. Budynas. And J. Nisbett, *Shigley's Mechanical Engineering Design*, *New York: McGraw-Hill*, 2006, pp. 107-108, 8th Ed.

[6] R. F. Gibson, *Principles of Composite Material Mechanics*, *New York: McGraw-Hill*, 1994.

[7] Kaw, A. K., *Mechanics of Composite Materials*, *New York: Taylor and Francis*,2006, 2nd Ed.

[8] L. P. Kollar and G.S. Springer, Mechanics of Composite Structures, *Cambridge University Press*, 2003.

[9] A. Baker, S. Dutton and D. Kelly, Composite Materials for Aircraft Structures, *AIAA Education Series*, 2nd Ed., 2004.

[10] A. Önder, *First Failure Pressure of Composite Pressure Vessels*, *Master Thesis*, Dokuz Eylul University, 2007.

[11] E. J. Heren, *Mechanics of Materials 2*, Great Britain: B.H., 1997, 3rd Ed..

[12] R. G. Budynas, *Advanced Strength and Applied Stress Analysis*, 2nd Ed., *New York: McGraw-Hill*, 1999, pp. 348–352.

[13] Ugural, A. C., and Fenster, S.K., *Advanced Strength and Applied Elasticity*, *New Jersey: Prentice Hall*, 4th Ed., Jan.2003.

[14] S. Bhaduri, *Pressure Cylinders*, *New York: McGraw-Hill*, Ch. 39, pp. 1–21, 2004.

[15] T. Ranov, and Park, R., On the numerical value of the Tangential Stress on Thick Walled Cylinders, *J.Appl. Mech.*, March 1953.

[16] L. Wolf, M. S. Kazimi, N. E. Todreas, Introduction to Structural Mechanics, *M.I.T., Department of Nuclear Engineering*., March 2003.

[17] G. H. Majzoobi and A. Ghomi, Optimization of Compound Pressure Cylinders, *J. A. M.M.E.*, Vol.15, 2006, pp. 135-145.

[18] A. A. Miraje and S. A. Patil, Minimization of material volume of three layer compound cylinder having same materials subjected to internal pressure, *J. I.J.E.S.T.*, Vol.3, No.8, 2011 pp. 26-40.

[19] M. P. Nemeth and M. M. Mikulas, *Simple Formulas and Results for Buckling-Resistance and Stiffness Design of Compression-Loaded Laminated-Composite Cylinders*, *NASA ,TP-2009-215778*, Aug. 2009.

[20] B. F. Tatting, *Analysis and Design of Variable Stiffness Composite Cylinders*, *P.H.D.*, Virginia Polytechnic Institute, 1998.

[21] D.O.D., Ceramic Matrix Composites, *MIL-HDBK-17-5*. Vol.5, Jun.2002, pp. 1-245.

[22] E. J. Heran, *Mechanics of Materials 1: An Introduction to the Mechanics of Elanstic and Plastic Deformation Solids and Structural Materials*, B.H.,Ch.9., 3rd Ed., 2001, pp. 198-213.

[23] R. K. Kunz, *Composite Reinforcement of Cylindrical Pressure Vessels*, *MAE 661 – Laminated Composite Materials Course' notes*, Mercer University, 2008.

[24] Nagesh, Finite-element Analysis of Composite Pressure Vessels, *Defense Science Journal*, Vol. 53, No. 1, 2003, pp. 75-86.

[25] J. M. Staniszewski, T. A. Bogetti, M. Keefe and B. Powers, An Improved Design Methodology for Modeling Thick-Section Composite Structures Using a Multiscale Approach, A.R.L., 2012, pp. 1-112,.

[26] S. Gohari, A. Golshan and A. Ayob, Theoretical Analysis and Finite Element Simulation of Behavior of Laminated Hemispherical GRP Dome Subjected to Internal Pressure, *International Conference on Computer and Software Modeling*, vol.14, 2011, pp. 111-117.

[27] Z. M. Kabir, Finite element analysis of composite pressure vessels with a load sharing metallic liner, *Journal of Composite Structures*, Vol. 49, 2000, pp. 247-255.

[28] J. S. Park and C. S. Hong, Analysis Of Filament Wound Composite Structures Considering The Change of Winding Angles Through The Thickness Direction, *Journal of Composite Structures*, Vol. 55, 2002, pp. 63-71.

[29] K. A. Roy, Strength Analysis and Design of Multilayered Thick Composite Spherical Pressure Vessels, *W.R.D.C.*, 1991, pp. 1-45.

[30] Zu, L., *Design and Optimization of Filament Wound Composite Pressure Vessels*, *MSc.Thesis*, Netherlands – BOX-Press, Ch.12, 2012, pp.195-216.

[31] Lekhnitskii S. G., Anisotropic plates, *New York: Gordon and Breach*, 1968. Translated by S. W. Tsai and T. Cheron.

[32] S. G. Lekhnitskii, *Theory of elasticity of an anisotropic elastic body, San Francisco: Holden-Day*, *Inc.*; 1963. Translated by P. Fern.

[33] I. Tsukrov and B. Drach, Elastic deformation of composite cylinders with cylindrically orthotropic layers, *Journal of Composite Structures*, Vol. 47, 2010, pp. 25-33.
[34] S. M. Shakib, *Analysis of composite laminated structures*, Emam Hossein University Press, 1986.
[35] S. S. Kumar and A. S. Kumari., Design and Failure analysis of Geodesic Dome of a Composite Pressure Vessel, *I.J.E.R.T.*, ISSN: 2278-0181, Vol. 1, Iss. 7, Sep. 2012.
[36] S. Bhavya, P. Ravi Kumar and Sd. Abdul Kalam., Failure Analysis of a Composite Cylinder, *I.O.S.R-J.M.C.E*, ISSN: 2278-1684, Vol. 3, Iss. 3, 2012, pp. 1-7.

Appendix

Table A.1. American & European Pressure Vessels Standards.

No.\Standard	American Boiler and Pressure Vessel Code	European Standards
1	ASME BPVC Sec. I - Power Boilers	EN 13445 - Unfired Pressure Vessels
2	ASME BPVC Sec. VIII Div. 1 - Pressure Vessels	PD 5500 - Unfired fusion welded pressure vessels
3	ASME BPVC Sec. VIII Div. 2 - Pressure Vessels (alternative rules)	
4	ASME BPVC Sec. VIII Div. 3 - Pressure Vessels (high pressure vessels)	
5	ASME BPVC Sec. X - Fiber Reinforced Pressure Vessels	

Table A.2. Property comparison from Ref. [10]

Material *	Density (g/cc)	Tensile Strength (MPa)	Tensile Modulus (MPa)	Specific Tensile Strength (10^3 m)
Filament Wound Composite	1.99	1034	31.02	52.96
Aluminium 7075-T6	2.76	565	71.01	20.87
Stainless Steel -301	8.02	1275	199.94	16.20
Titanium Alloy (Ti-13 V-12 Cr-3 Al)	4.56	1275	110.3	28.50

*For unidirectional composites, the reported modulus and tensile strength values are measured in the direction of fibers.

(Source: C-K Composites, Mount Pleasant, PA)

Table A.3. Filament wound products: Applications Vs. Resin systems used from Ref. [10]

Industry	Typical Application	Typical Resin Systems
Corrosion	• Underground Storage Tanks • Aboveground Storage Tanks	Polyester (Ortho- and Iso-phthalic), Vinyl Ester
	• Piping Systems • Stack Liners • Ducting Systems	Polyester (Ortho- and Iso-phthalic), Vinyl Ester, Epoxy, Phenolic
Oilfield	• Piping Systems • Drive Shafts • Tubular Structures	Epoxy, Phenolic
Paper and Pulp	• Paper Rollers • Piping Systems • Ducting Systems	Vinyl Ester, Epoxy
Infrastructure and Civil Engineering	• Column Wrapping • Tubular Support Structures • Power Poles • Light Standards	Polyester (Ortho- and Iso-phthalic), Vinyl Ester, Epoxy
Commercial Pressure Vessels	• Water Heaters • Solar Heaters • Reverse Osmosis Tanks • Filter Tanks • SCBA (Self-Contained Breathing Apparatus) Tanks • Compressed Natural Gas Tanks	Polyester (Ortho- and Iso-phthalic), Vinyl Ester, Epoxy
Aerospace	• Rocket Motor Cases • Drive Shafts • Launch Tubes • Aircraft Fuselage • High Pressure Tanks • Fuel Tanks	Epoxy, Bismaleimide (BMI), Phenolic, Vinyl Ester
Marine	• Drive Shafts • Mast and Boom Structures	Epoxy
Sports and Recreation	• Golf Shafts • Bicycle Tubular Structures • Wind Surfing Masts • Ski Poles	Epoxy